Model for the propagation of pulses and mode scrambling in a real POF with structural imperfections

J. Arrue [1], J. Zubia[1], G. Durana[1], J. Mateo[2], and M. Lopez-Amo[3]

University of (1) the Basque Country, (2) Zaragoza, (3) Navarra, Spain

Abstract

Plastic optical fibers (POFs) can be appropriately bent to provoke mode scrambling. Such techniques allow the mode equilibrium to be achieved in shorter lengths. On the other hand, computer programs designed for the theoretical study of POFs by means of the ray tracing method do not usually take into account structural imperfections in the POF. Therefore, in this paper we present a theoretical model to determine the propagation of light in a real POF with structural imperfections and we employ it to simulate the influence of bends at the beginning of the optical link.

1. Introduction

POFs are especially advantageous for short-distance communications links, in which ease in connection and mechanical flexibility are usually important parameters. Different types of POFs can be employed depending on the application. While the new graded-index POFs allow very high data rates to be achieved, the traditional step-index POFs are especially easy to handle, since they facilitate the light coupling from the light source, due to their large core diameter and high numerical aperture. Therefore, accurate characterization of a POF is critical in selecting the proper fibers for any particular use. However, in short POFs the equilibrium mode distribution (EMD) condition is not yet completely achieved, so the experimental results can strongly depend on the input light power distribution [1]. On the other hand, the structural imperfections present in all commercial fibers would serve to reach the EMD condition after light travels a sufficiently long distance, as a result of the diffraction of light by microscopic anomalies in the fiber core, and, in the case of SI POFs, also because of non-ideal reflections at the core-cladding interface. However, the use of mode scramblers reduces the coupling length considerably, thus allowing the experimental results to be approximately independent of the input light distribution.

One of the contributions of this work has been the attainment of a propagation model that includes the microscopic anomalies in the fiber core and core-cladding interface in SI POFs. In addition, different combinations of bends and straight fiber sections are analyzed with this model, for the sake of a better understanding of the internal performance of mode scramblers. Although mode scramblers have been traditionally made with SI POFs, we also analyze the possibility of employing a GI POF.

The propagation model has been developed on the basis of the ray tracing method, by introducing random alterations in the ray paths at the reflection points and also in the bulk material. Specifically, the trajectory of each ray inside the core is regularly modified every certain distance along its propagation direction. This distance represents an average length traveled by the ray before it changes its path, as a consequence of its interaction with any of the randomly distributed microscopic fluctuations in the refractive index. We will call this distance *mean free path*. On the other hand, the angular alterations in the reflection directions at the core-cladding interface stand for the fact that the interface is not completely smooth.

In Section 2 we explain the model developed for the propagation of light in a real SI POF, and how the computational parameters have been adjusted. In Section 3, some possible mode-scrambling configurations are analyzed. In all of them, the POF is bent around several cylindrical rods arranged in different relative positions. Specifically, we calculate the progressive light power redistribution along the different constituent straight and bent sections of our investigated set-ups. For this purpose, our model for light propagation is used to obtain the successive far fields that would be obtained from each of the successive fiber sections in the absence of the following ones. From the analysis we arrive at some conclusions regarding the influence of parameters such as the distance between rods, the number of rods and the arc lengths.

2. Model for the propagation of light in a real SI POF

Our model has been developed step by step in several stages, introducing successive changes towards a more advanced and comprehensive model. The values assigned to the adjustable simulation parameters have always been chosen to fit the experimental results as well as possible. The fiber used for our simulations was SUPER ESKA SH 40001 (Mitsubishi Rayon Co., Ltd.). Its core and cladding refractive indices are n_1=1.492 and n_2=1.402 respectively, which corresponds to a numerical aperture of 0.51, and its fiber diameter is 1 mm.

To develop our model, a computational program based on the ray tracing method and capable of evaluating output light power distributions and far fields was prepared. This program allows to deal with consecutive straight and bent fiber sections. It also includes the possibility of simulating different types of light sources located at different distances from the fiber input and orientated at different possible angles.

In the first stage, we checked the influence of structural imperfections on the far field of the output of a straight POF. The idea was to launch parallel rays making a certain angle θ with the fiber symmetry axis. If the theoretical result in the absence of mode mixing is computed, two distinct narrow peaks appear in the far field, centered at the angles $+\theta$ and $-\theta$. However, when the corresponding far field is measured experimentally these peaks broaden and even overlap each other, due to mode mixing.

The computed far field is evaluated from the output power distribution, that is, from the knowledge of the exact position at which each ray crosses the output end and its orientation and associated power. To specify this information we use five variables. On the one hand we employ a variable to store the remaining power after applying the corresponding reflection coefficients R at the reflection points (one possibility is to

assume R=1 for tunneling rays and bound rays and R=0 for refracting rays, as we discuss later). On the other hand, we use two polar coordinates for the position and two angles for the orientation: an axial angle with the fiber symmetry axis and an azimuthal angle defining the specific orientation in the cone of all possible rays for the mentioned axial angle.

Fig. 1 shows the far field intensity measured experimentally when a 6 meter POF was illuminated uniformly at the input end by a HeNe laser source, in such a way that the incident light beam made an angle $\theta = 20°$ in air with the fiber symmetry axis. We can note that, instead of obtaining two narrow peaks at +20 and –20 degrees, these peaks have broadened so much that they even overlap each other.

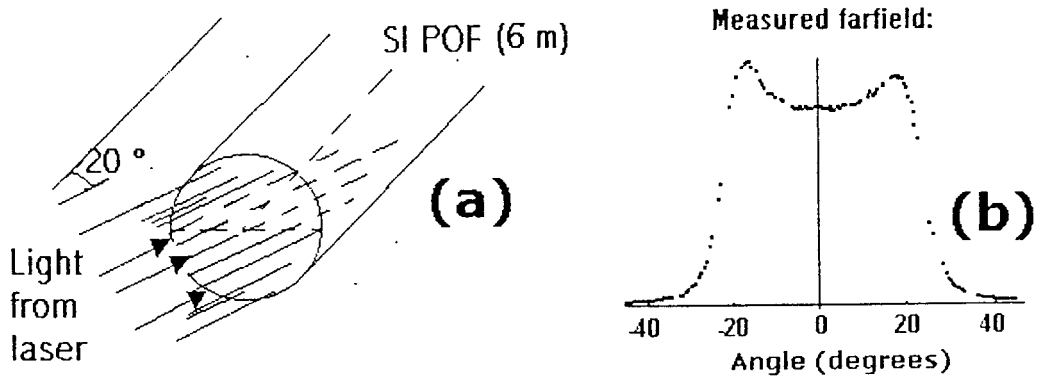

Figure 1. (a) Light launching conditions. (b) Broadening of the measured far field power distribution in a real POF.

In the second stage, a first model with structural imperfections was developed, so as to achieve the broadening in the peaks mentioned above. In this model, light rays followed straight paths inside the core, but their direction was deflected away from that predicted by Snell's law when they reached the core-cladding interface. The deviation from the theoretical reflection angle was modeled by means of a Gaussian probability function centered around the incidence angle. Specifically, the new reflection angle (x) differed from that given by Snell's law (x_O) in a random value given by following expression:

$$y = e^{\frac{(x-x_O)^2}{2\sigma^2}} \qquad (1)$$

where y is a random number in the range between 0 and 1 and σ represents the width of the Gaussian. At the beginning, only the axial angle was changed in this way, but in the last model both the axial and the azimuthal angle are considered.

With this model the region between the two peaks (see Fig. 1-b) was too low in comparison with the experimental measurements. For this reason, the possibility of using a relative σ, that is, of varying the value of σ as a function of the incidence angle

was also checked. A first approach was the introduction of a percentage of relative σ from the keyboard, for example 10%. This would mean that σ for an incident angle of 20° would be 2°, whereas it would be 0.1° for an incident angle of 1°. The problem was that, for small values of the percentage, the amount of rays with an axial angle very close to 0° did not increase, while, for large values, σ became too big for the largest incidence angles. In consequence, instead of using a fixed percentage, in the following models the value of the relative σ, in the case of using a relative one, will be obtained by using a multiplicative factor that depends on the angle, for example $\sigma = angle * e^{-angle}$.

Another problem of this first model was that it did not serve to model the broadening when the laser beam was parallel to the fiber axis, even though the divergence angle of the laser was introduced (typically, 0.0578°, or 1 mrad). Therefore, in a third stage, the concept of mean free path already commented was introduced. Specifically, every certain distance, for example 1 mm, the ray path was modified. The deviation from the original angle was also modeled by means of a Gaussian probability function of width σ_{vol}. In addition, we maintained the Gaussian deviations at the core-cladding interface, with a value σ_{surf} that could be different from σ_{vol}. Both values were adjusted by comparing the computational results with the experimental ones for several fiber lengths. In a first attempt the mean free path was considered in the direction of the fiber axis, instead of along the ray path. Once we introduced the mean free path along the ray direction, we obtained very similar optimum values for σ_{vol} and σ_{surf} for each of the fiber lengths considered.

In a fourth stage, we began to take into account the azimuthal angle for the first time, both in the bulk material and on the surface, since all the deviations in the previous stages were applied only to the axial angle. Therefore, in this last model, we have four different types of σ, whose values have been adjusted experimentally, yielding the following results:

$\sigma_{\mathbf{vol\text{-}azimuthal}} = 0.05$ (absolute)
$\sigma_{\mathbf{vol\text{-}axial}} = 0.1$ (relative)
$\sigma_{\mathbf{surf\text{-}azimuthal}} = 0.05$ (absolute)
$\sigma_{\mathbf{surf\text{-}axial}} = 0.05$ (absolute)

We can note that $\sigma_{\mathbf{vol\text{-}axial}}$ is relative, or, in other words, it is a function of the angle. Specifically, the new axial angle is equal to the old one, plus or minus (randomly) the increment in the angle obtained from (1) multiplied by e^{-angle}. The other values of σ do not depend on the angle.

In this last model the reflection coefficients *R* at the reflection points have been assumed to be *R*=1 for tunneling rays and bound rays and *R*=0 for refracting rays. This means that tunneling rays are not neglected, because in practice they tend to attenuate very little at each reflection point, and also that refracting rays are eliminated, because they tend to attenuate very much at each reflection point [2]. Another reason not to neglect tunneling rays is that, when we tried considering only bound rays, the

experimental tails that appear at axial angles greater than the complementary critical angle did not appear.

3. Some possible mode-scrambling configurations and conclusions

We will now apply the above described computational model to simulate and compare the possible scrambling properties of several configurations, such as several turns around a single cylindrical rod, a series of serpentine bends in the beginning of the fiber (Fig. 2-a), an alternate succession of short straight and curved fiber sections (Fig. 2-b), or two parallel cylindrical rods with a center to center distance slightly greater than the diameter of the rods (Fig. 2-c). The configurations of Figs. 2-b and 2-c were proposed in references [3] and [4] respectively, but our purpose is to analyze the successive far fields, like those that would result from points 0, 1, 2, ..., 9 of Fig. 2-b for example, in order to get a better understanding of the internal performance of such configurations. For the same purpose, in the case of Fig. 2-b we will also vary the distances d_2 and d_4.

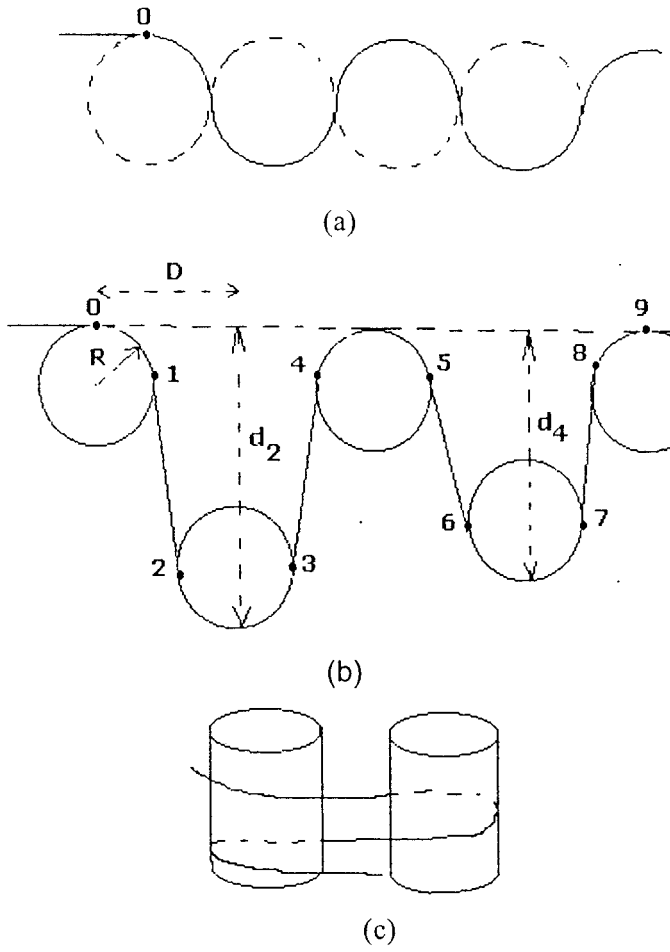

Figure 2. Some possible mode-scrambling configurations.

For the sake of comparison we will submit all the scramblers to the same types of illumination. For example, let us first simulate 3 cm of straight fiber illuminated uniformly by a laser, as in Fig. 1, but with θ=10°. The simulated far field in the plane of the bend is shown in Fig 3. One of the characteristics that the configurations shown in Fig. 2 have in common is that the fiber is curved alternatively around concave and convex circular arcs, no matter whether there are straight sections between the curved ones or not. The reason of such alternation in the convexity can be better understood by calculating the corresponding far fields in the plane of the bend when the POF is bent with different numbers of turns around a single rod of radius R (Fig. 4).

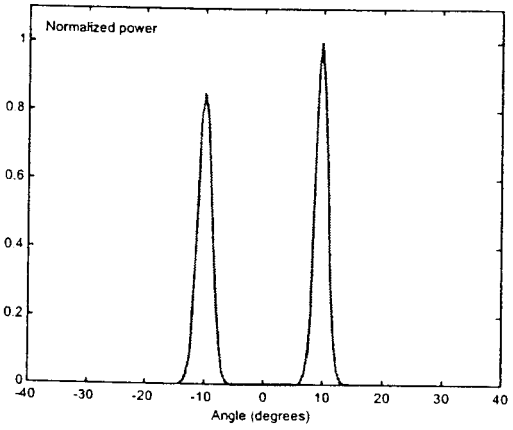

Figure 3. Simulated far field for 3 cm of straight fiber illuminated uniformly by a laser, as in Fig. 1, with θ=10°.

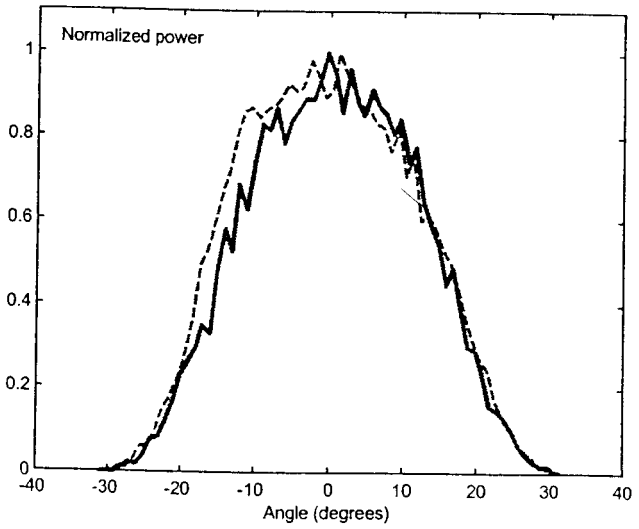

Figure 4. Far fields in the plane of the bend when the POF is bent with different numbers of turns around a single rod of radius R=10 mm: 1 ½turns: dashed line; 5 turns: continuous line.

We can note that no significant change in the far field is obtained because of increasing the number of turns, since an equilibrium for the curve has been reached, so this configuration is usually used in combination with other rods, to be able to achieve further improvements in the far field. The desired result is a uniform overfilled angular distribution of the power, independently of the radiation properties of the light source and its alignment, which is the function of a mode scrambler [5]. In fact, the ideal far field of a step-index fiber with simple geometric optics would be a rectangle, in the absence of significant material attenuation and scattering [6]. On the other hand, the idealized far field from a fully excited graded-index fiber would have a different shape, with the power more concentrated in the center than at the sides [7]

Now, if we repeat the calculations with the same launching conditions and the same bend radii for the rods but with the configuration of Fig. 2-a, we can see that with two consecutive rods the far field is much more similar to the desired rectangle than with only one rod. However, the improvement becomes slower as we increase the number of rods

If we check the configuration of Fig 2-b for three different sets of distances d_2 and d_4, maintaining the values of D=25 mm and R=10 mm suggested in [3] for the optimal scrambler, we obtain that the far field tends to be rectangular in shape, but it improves very slowly in all cases from the fourth rod. The far fields from points 0, 2 and 9 of Fig-2b are plotted in Fig. 5 for d_2=110 mm and d_4=86 mm. The longer these distances, the longer the straight sections and the less pronounced the peaks are in their corresponding far fields, For the same scrambler, the far field from point 2 and the following ones tend to be very similar independently of the launching angle θ. The results have been simulated with more than 100.000 rays at the beginning, which proved to be enough (approximately the same results with 100.000 rays and with 500.000 were obtained).

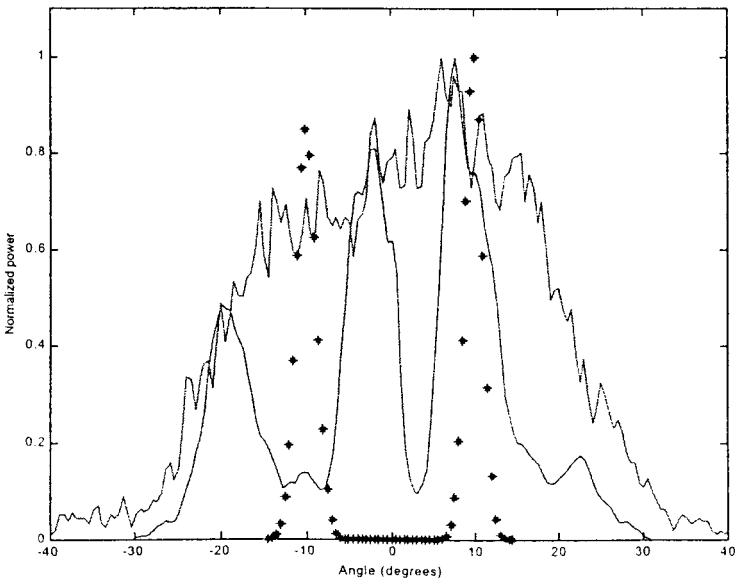

Figure 5. Far fields from points 0 (dotted), 2 (dashed) and 9 (continuous) of Fig-2b

With the scrambler of Fig 2-c a far field close to a rectangle is very soon achieved (only with two bends), but increasing the number of bends improves the result very slowly.

The configuration of Fig. 2-b could also serve as a mode scrambler for GI POFs,. If we multiply all the lenghs and radii considered for Fig. 5 by two, in order to maintain the relatively low losses, we obtain that the far fields at points 0 and 9 are these shown in Fig. 6.

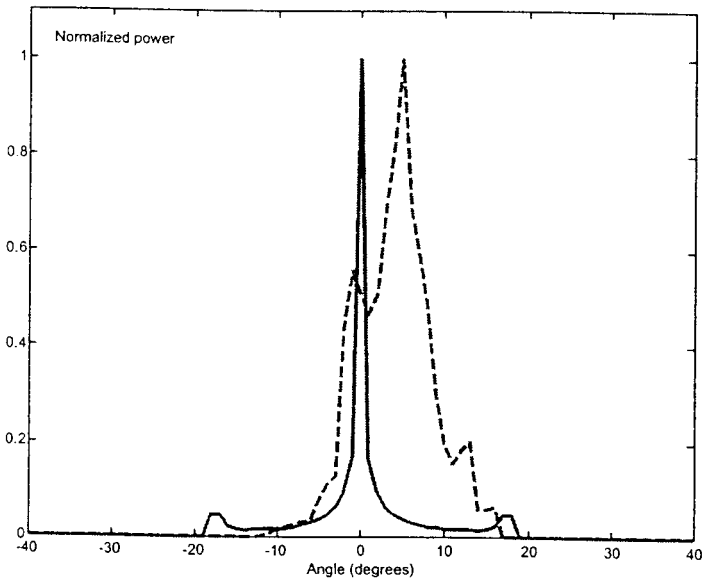

Figure 6. Far fields from points 0 (continuous) and 9 (dashed) of Fig-2b, but for a GI POF

4. References

[1] G. Jiang, R. F. Shi, and A. F. Garito, "Mode Coupling and Equilibrium Mode Distribution Conditions in Plastic Optical Fibers", IEEE Photon. Tech. Lett., Vol. 9, No. 8, August 1997.

[2] J. Arrue, J. Zubia, G.Fuster, and D. Kalymnios, "Light power behaviour when bending plastic optical fibres", IEE Proc.-Optoelectron., Vol. 145, No. 6, pp. 313-318, Dec. 1998.

[3] R. Attia, S. Jarboui, M. Machhout, A. Bouallegue, and J. Marcou, "Modal scrambler for polymer optical fiber", Proc. Fifth International Conference on Plastic Optical Fibers and Applications POF'95, pp. 30-31, 1996.

[4] G. Fuster-Martinez, D. Kalymnios, and I. W. Rogers, "Mode stripping and scrambling with step-index high NA POF", Proc. Fifth International Conference on Plastic Optical Fibers and Applications POF'95, pp. 36-37, 1996.

[5] F. C. Allard, "Fiber Optics Handbook for Engineers and Scientists" (McGRAW-HILL)

[6] Nürnberg POF Application Center, "Modelation and Simulation of Plastic Optical Fibers", May 2001.

[7] C. Hentschel, "Fiber Optics Handbook", Hewlett-Packard, March 1989.